

# ULRR

## Enzymatic biofuel cells for self-powered, controlled drug release

Item Type	Article
Authors	Xiao, Xinxin;Mc Gourty, Frank;Magner, Edmond
Citation	Journal of the American Chemical Society, 2020, 142, (26), pp. 11602–11609
Publisher	American Chemical Society
Download date	2026-05-15 07:04:01
Item License	<a href="https://creativecommons.org/licenses/by-nc-sa/4.0/">https://creativecommons.org/licenses/by-nc-sa/4.0/</a>
Link to Item	<a href="https://doi.org/10.34961/researchrepository-ul.27201933">https://doi.org/10.34961/researchrepository-ul.27201933</a>

# Enzymatic Biofuel Cells for Self-Powered, Controlled Drug Release

Xinxin Xiao,<sup>†,§</sup> Kieran Denis McGourty<sup>†,‡</sup> and Edmond Magner<sup>†,‡</sup>

<sup>†</sup>Department of Chemical Sciences and Bernal Institute, University of Limerick, Limerick, Ireland

<sup>§</sup>Department of Chemistry, Technical University of Denmark, Kongens Lyngby 2800, Denmark.

<sup>‡</sup>Department of Chemical Sciences and Health Research Institute, University of Limerick, Limerick, Ireland

**ABSTRACT:** Self-powered drug delivery systems based on conductive polymers (CPs) that eliminate the need for external power sources, are of significant interest for use in clinical applications. Osmium redox polymer mediated glucose/O<sub>2</sub> enzymatic biofuel cells (EBFCs) were prepared with an additional CP-drug layer on the cathode. On discharging the EBFCs in the presence of glucose and dioxygen, model drug compounds incorporated in the CP layer were rapidly released with negligible amounts released when the EBFCs were held at open circuit. Controlled and *ex situ* release of three model compounds, ibuprofen (IBU), fluorescein (FLU) and 4',6'-diamidino-2-phenylindole (DAPI), was achieved with this self-powered drug release system. DAPI released *in situ* in cell culture media was incorporated into retinal pigment epithelium (RPE) cells. This work demonstrates a proof-of-concept responsive drug release system that may be used in implantable devices.

## INTRODUCTION

Enzymatic biofuel cells (EBFCs) consisting of sugar-oxidising bioanodes and oxygen-reduction biocathodes can harvest electricity from chemical energy.<sup>1-3</sup> When consuming a fuel, such as glucose, that is present in physiological fluids<sup>4</sup>, membrane-less EBFCs possess significant potential for use as activators for implantable medical devices. A significant advantage of EBFCs lies in the continuous supply of fuel, as opposed to batteries, which need replacement.<sup>5-7</sup> Significant challenges such as operational stability together with mismatches between the output voltages of EBFCs (typically below 1 V) and the minimum activation input voltage required to operate many microelectronic devices (generally in the range 1-3 V with recent reports describing lower voltages of 0.5 V<sup>8</sup>) hinder the application of EBFCs as direct and independent power sources<sup>6</sup>.

A possible solution is to develop self-powered devices<sup>9</sup> that utilise EBFCs directly to enable functions such as biosensing<sup>10-11</sup> and self-sustained pulse generators.<sup>12-13</sup> Responsive polymer based drug delivery systems have gained significant attention in recent years.<sup>14-16</sup> Self-powered release systems have been described, with the potential to act as “sense-act-treat” devices.<sup>17-20</sup> Such systems generally use abiotic cathodes such as a Fe<sup>3+</sup>-cross-linked alginate polymer loaded with drug molecules. Reduction of Fe<sup>3+</sup> to Fe<sup>2+</sup>, by a coupled bioanode in the presence of sugars results in dissolution of the polymer releasing the entrapped species.<sup>18-19</sup> However, alginate polymers are unstable at high pH and the release of Fe<sup>2+</sup> (or other metal ions) may not be desirable. Nishizawa et al. developed an iontophoresis patch that utilised an EBFC for the transdermal delivery of ascorbyl glucoside and rhodamine B.<sup>21</sup> Such an approach is restricted to transdermal applications and is not suitable for implantable applications.

On account of their high electrical conductivity, mechanical stability and ease of preparation, conducting polymers (CP) are used in a range of applications that include light emitting diodes, capacitors, electrochromic devices, actuators, etc.<sup>22-23</sup> The preparation of the polymers entails oxidation of a monomer species, followed by a chain reaction to form the CP. Due to the charged nature of the CP, counterions are incorporated into the polymer to balance the charge on the polymer.<sup>23-24</sup> On reduction of the polymer, these dopant ions are subsequently expelled. Typically, the dopants are anionic or cationic components of the electrolyte. Other charged species present in the electrolyte solution can also be incorporated as dopants in the polymer and then released on reduction of the polymer. Galvanic cell based self-powered drug delivery

systems<sup>25</sup> consisting of a conductive polymer (CP) cathode, with the drug incorporated within the polymer matrix, and a metal (e.g. Mg and Zn) anode with a very negative half-cell potential have been described.<sup>26</sup> Reduction of the CP film by the metal anode leads to the expulsion of the incorporated drug. Such devices can suffer the disadvantage of release of metal ions as described above and the inability to pause oxidation of the metal anode,<sup>26</sup> diminishing the capacity to regulate the rate of release.

In this report, we describe a versatile strategy to prepare a self-powered drug release system based on EBFCs which has the potential to be used *in vivo*. A membrane-less glucose/O<sub>2</sub> EBFC, that can generate electricity from glucose and dioxygen, was prepared using a [Os(2,2'-bipyridine)<sub>2</sub>(polyvinylimidazole)<sub>10</sub>Cl]<sup>+2+</sup> (Os(bpy)<sub>2</sub>PVI) mediated glucose oxidase (GOx) anode and a Os(bpy)<sub>2</sub>PVI mediated bilirubin oxidase (BOx) cathode (**Scheme S1**).<sup>12</sup> Thin nanoporous gold (NPG, pore size: ca. 30 nm, roughness factor: 7-8) films with a thickness of ca. 100 nm were used as biocompatible and conductive electrodes.<sup>12, 27-29</sup> CP layers were electropolymerized onto the NPG/Os(bpy)<sub>2</sub>PVI-BOx cathodes in the presence of model drugs. Controlled release of the drugs was switched “on” in the presence of glucose and dioxygen and switched “off” at open circuit. This proposed approach is unique and avoids the limitations outlined above with self-powered electrically triggered drug release systems (see summary in **Table S1**). No external electrical input is required for the controlled drug release process described here. Two anionic (ibuprofen (IBU) and fluorescein (FLU)), and a cationic species (4',6'-diamidino-2-phenylindole (DAPI)) were examined (**Scheme S2**). IBU is one of the most-widely employed non-steroidal anti-inflammatory drug and was selected as a model drug to demonstrate the feasibility of the approach. FLU and DAPI were selected as model fluorescent compounds and DAPI in particular with due to its ability to stain cell nuclei. Controlled release of the three model compounds, was successfully demonstrated, illustrating the general nature of the approach.

## RESULTS AND DISCUSSION

**Controlled Release of Anionic Drug Ibuprofen (IBU).** IBU can be doped into poly(3,4-ethylenedioxythiophene) (PEDOT) as negatively charged doping ions.<sup>30</sup> Previous work<sup>30</sup> has shown that IBU can be released in a controlled manner by applying a negative potential to reduce PEDOT which undergoes a de-doping process (**Eq. S1**). Electrically triggered drug release is simple and versatile as it enables the on-demand

release of drugs with the concomitant requirement for intermittent dosage of medications as needed. However, *in situ* applications are limited when external power input is needed. In the proposed approach, a PEDOT-IBU layer was electrodeposited onto a NPG/Os(bpy)<sub>2</sub>PVI-BOx biocathode (Fig. 1A, Fig. S1). The reduction of dioxygen at the cathode occurred with concomitant reduction of the outer PEDOT layer releasing IBU into solution. A similar methodology was applied for the self-powered release of the commonly used fluorophores FLU (Fig. 2A) and DAPI (Fig. 3A).

Fig. 1B shows the biocatalytic dioxygen-reduction response of the NPG/Os(bpy)<sub>2</sub>PVI-BOx/PEDOT-IBU biocathode. The electrode exhibited a pair of redox peaks in N<sub>2</sub> bubbled PBS, with a midpoint potential ( $E_m$ ) of 0.191 V vs. SCE, assigned to the redox behavior of the Os<sup>2+/3+</sup> couple. The faradaic response of Os<sup>2+/3+</sup> was superimposed on the pseudo-capacitive current of PEDOT (Fig. S2). On comparison of the cyclic voltammograms (CVs) of NPG/Os(bpy)<sub>2</sub>PVI-BOx/PEDOT-IBU and NPG/Os(bpy)<sub>2</sub>PVI-BOx (Fig. S2) the capacitance of the latter increased from 415 to 570  $\mu\text{C cm}^{-2}$ , indicative of the formation of an additional PEDOT-IBU layer. In an air-equilibrated solution, electrocatalytic reduction of oxygen commenced at 0.327 V vs. SCE, reaching a maximum net catalytic current density ( $j_{\text{net}}$ ) of  $15.8 \pm 0.4 \mu\text{A cm}^{-2}$  at 0.121 V, a value lower than that of the NPG/Os(bpy)<sub>2</sub>PVI-BOx electrode ( $31.5 \pm 2.3 \mu\text{A cm}^{-2}$  at 0.178 V) (Fig. S2). The presence of IBU showed no inhibitory effects on the activities of GOx and BOx (Fig. S3). Enzymatic assay of immobilized BOx after coating with the second PEDOT-IBU layer showed a somewhat lower activity (details in Experimental Section). As observed with the electrochemical response, this decrease can be ascribed to O<sub>2</sub> diffusional limitations arising from the additional polymeric layer. Scanning electron microscopic (SEM) (Fig. S4) and transmission electron microscopic (TEM) (Fig. S5) and atomic force microscopic (AFM) (Fig. S6) images of the bare and modified electrodes indicate that there was a buildup of polymer layers on the electrode surface. Although it was not possible to distinguish between the two layers using TEM, the thickness of the coating layer on Os(bpy)<sub>2</sub>PVI-BOx/PEDOT-IBU ( $6.7 \pm 1.4 \text{ nm}$ ) was larger than that of Os(bpy)<sub>2</sub>PVI-BOx ( $3.7 \pm 0.4 \text{ nm}$ ) (Fig. S5). Using Fourier transform infrared spectroscopy (FTIR) (Fig. S7), the first coating layer of Os(bpy)<sub>2</sub>PVI-BOx showed bands at  $1455 \text{ cm}^{-1}$  (C=C stretching) and  $1418 \text{ cm}^{-1}$  (imidazole cycle stretching) corresponding to the presence of polyvinylimidazole. The appearance of a band at  $1385 \text{ cm}^{-1}$  band that was not present with the Os(bpy)<sub>2</sub>PVI-BOx modified electrode can be assigned to C=C stretching in the thiophene ring confirmed the successful generation of the second PEDOT-IBU layer.

The lower  $j_{\text{net}}$  was attributed to the reduced rate of mass transport of O<sub>2</sub> to BOx due to steric hindrance by the PEDOT layer. The decrease in the flux was verified by a control experiment using a PEDOT layer, without IBU doping on NPG/Os(bpy)<sub>2</sub>PVI-BOx, where a significant decrease (72%) in the catalytic response was also observed at 0 V vs. SCE (Fig. S3B). This is consistent with previous reports where NPG electrodes modified with additional layers displayed lower responses.<sup>12, 31</sup> CVs of NPG/Os(bpy)<sub>2</sub>PVI-GOx displayed (Fig. 1C) a pair of redox peaks with an  $E_m$  of +0.188 V vs. SCE in a blank solution with no substrate, and a  $j_{\text{net}}$  of  $97.5 \pm 9.1 \mu\text{A cm}^{-2}$  at +0.201 V vs. SCE and an onset potential of -0.055 V vs. SCE in the presence of 10 mM glucose. In an air-equilibrated solution containing 10 mM glucose, the assembled EBFC(1) registered an open-circuit voltage (OCV) of 0.377 V and a maximum power density ( $P_{\text{max}}$ ) of  $1.35 \mu\text{W cm}^{-2}$  at 0.124 V (Fig. 1D). The obtained OCV was in agreement with the difference between the onset potentials of the bioanode and the biocathode. The potential difference between two electrodes modified with the same Os polymer is based on the Nernstian potential difference arising from differing ratios of oxidised and reduced Os polymer at the two electrodes.<sup>32</sup> Due to the mediated biocatalytic reactions (glucose oxidation and oxygen reduction) at the bioanode and biocathode, the ratio of oxidised and reduced

Os polymer on each electrode will be different, establishing a potential difference between the two electrodes, i.e. OCV of an EBFC. The use of the same mediator for EBFCs has been described in a number of studies.<sup>12, 33-34</sup> If required the OCV can be altered and improved by using two different redox polymers with redox potentials close to those of the enzymes. The power density of EBFC(1) is limited by the biocathode when the glucose concentration is over 3 mM, based on the fact that the catalytic current density of the bioanode (Fig. S8) is much higher than that of the biocathode (Fig. 1B). Considering the glucose concentration in plasma is typically 5 mM or higher, the power density of the EBFC is thus always limited by the biocathode. Thus, changing glucose concentrations (when above 3 mM) would not affect the drug release kinetics. EBFC(1) registered a half-lifetime of 9.2 h under continuous operation at 0.15 V in buffer (Fig. S9).

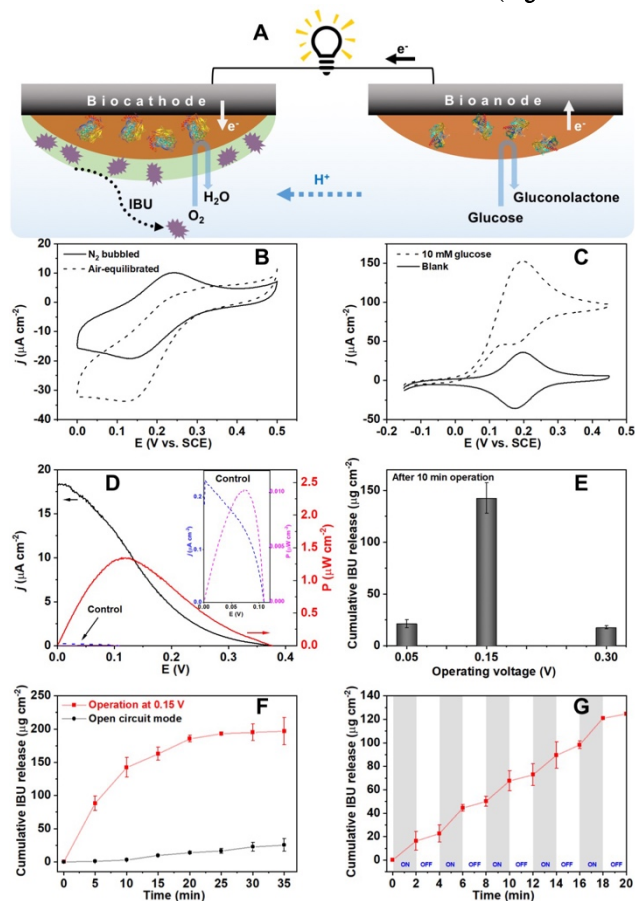


**Figure 1.** (A) Schematic illustration of controlled IBU release based on an EBFC(1); (B) Cyclic voltammograms (CVs) of the NPG/Os(bpy)<sub>2</sub>PVI-BOx/PEDOT-IBU biocathode (B) and NPG/Os(bpy)<sub>2</sub>PVI-GOx bioanode (C) in 0.1 M pH 7.0 phosphate buffer solution (PBS) at a scan rate of 5 mV s<sup>-1</sup>; (D) Power and current density profiles of the EBFC(1) consisting of a NPG/Os(bpy)<sub>2</sub>PVI-GOx bioanode and a NPG/Os(bpy)<sub>2</sub>PVI-BOx/PEDOT-IBU biocathode in air-equilibrated solution containing 10 mM glucose; (Inset of D) the control cell was composed of a NPG/Os(bpy)<sub>2</sub>PVI-GOx bioanode and a NPG/Os(bpy)<sub>2</sub>PVI/PEDOT-IBU cathode; (E) Cumulative amount of IBU released from the IBU loaded EBFC(1) operating at various voltages for 10 min; (F) Cumulative amount of IBU released by EBFC(1) operating at 0.15 V (red line) and at open-circuit mode (spontaneous release) (black line); (G) Cumulative amount of IBU released by EBFC(1) operating in “on-off” mode: with “on” representing a potential of 0.15 V and “off” the open-circuit mode.

EBFC(1) was discharged at a range of potentials (Fig. 1E) and the cumulative amount of IBU released was determined from the absorbance at 222 nm (Fig. S10). The optimal voltage for release of IBU was 0.15 V, similar to the voltage observed at  $P_{\max}$  (0.124 V) (Fig. 1D). The relationship between EBFC voltage and the voltages of the biocathode and bioanode is given by:  $E_{\text{cell}} = E_{\text{biocathode}} - E_{\text{bioanode}}$ . For  $E_{\text{cell}}$  potentials of 0.05, 0.15 and 0.3 V of EBFC(1), we examined the corresponding voltages for the biocathode (0.066, 0.12 and 0.25 V vs. SCE) and bioanode (0.016, -0.032 and -0.05 V vs. SCE), respectively (Table S2). The amount of IBU released from NPG/Os(bpy)<sub>2</sub>PVI-BOx/PEDOT-IBU biocathode solely in a three-electrode setup was monitored at 0.066, 0.12 and 0.25 V vs. SCE for 5 min, respectively. When the biocathode was operating at 0.12 V vs. SCE (Fig. S11), corresponding to conditions where the voltage of EBFC(1) was 0.15 V, the amount of IBU released was at a maximum. This is consistent with the data in Fig. 1B, where the biocathode registered a maximum current density at 0.12 V vs. SCE. This demonstrates that the results obtained with the biocathode in a three-electrode cell were consistent with those observed when operating EBFC(1) in a two-electrode cell. We thus can conclude that the optimal rate of release of IBU is obtained close to the voltage observed at  $P_{\max}$ , enabling more rapid de-doping of PEDOT-IBU, enhancing the rate of release of IBU.

The time profiles of release of IBU from the self-powered system at 0.15 V and at open-circuit are shown in Fig. 1F. The amount of drug loaded on the electrode was estimated to be  $570 \pm 32 \mu\text{g cm}^{-2}$ . Rapid IBU release occurred during the initial period of discharge (10 min), reaching an equilibrium value of  $197 \pm 20 \mu\text{g cm}^{-2}$  in ca. 30 min, corresponding to 35% release of the total load of IBU. This time frame is similar to that previously reported using a Pt electrode with a PEDOT/IBU layer where IBU was released on reduction of PEDOT with the maximum rate of release occurring at a potential of -0.5 V vs. Ag/AgCl.<sup>30</sup> In that system, release of IBU required the application of a potential bias from an external source. Os(bpy)<sub>2</sub>PVI-BOx has a midpoint potential of 0.191 V vs. SCE, while PEDOT can be reduced at a similar potential<sup>12,35</sup>, indicating that both Os(bpy)<sub>2</sub>PVI and PEDOT-IBU can be reduced by accepting electrons from the bioanode via the external circuit. The reduction of the PEDOT-IBU layer was confirmed by an increase in absorbance at 500 nm after operation of the EBFC<sup>36</sup> (Fig. S12). Although the detailed mechanism of operation has to be established, electron transfer (ET) between the underlying Os(bpy)<sub>2</sub>PVI and PEDOT-IBU layers was evident by (i) the successful electropolymerization of EDOT onto the Os(bpy)<sub>2</sub>PVI layer (Fig. S1) and (ii) CVs of NPG/Os(bpy)<sub>2</sub>PVI-BOx/PEDOT-IBU electrodes that showed faradaic peaks corresponding to the redox reaction of Os<sup>2+/3+</sup> superimposed on the charge/discharge capacitive currents of PEDOT (Fig. S2).

The amount of spontaneous release of IBU from NPG/Os(bpy)<sub>2</sub>PVI-BOx/PEDOT-IBU was not significant (12% of the amount at a potential of 0.15 V) (Fig. 1F) and can be attributed to the release of loosely-bound and physically-absorbed species. The use of longer washing/soaking times would clearly reduce this effect. This low level of spontaneous release provides evidence that release by EBFC(1) at 0.15 V was occurring in a controlled manner. An “on-off” operating sequence for EBFC(1) working alternatively at 0.15 V (2 min) and open-circuit (2 min) confirmed the controlled release of IBU, with an immediate decrease in the amount of IBU released during the “off” stages (Fig. 1G). As a control, a cell using the same anode, but with a NPG/Os(bpy)<sub>2</sub>PVI/PEDOT-IBU cathode without BOx (Fig. 1D), had an OCV of 0.109 V and a negligible  $P_{\max}$  of  $0.01 \mu\text{W cm}^{-2}$ , highlighting the requirement for BOx at the cathode. This data demonstrates that in the presence of BOx and the accompanying oxygen reduction reaction, a potential difference (i.e. OCV) is established between the cathode and the NPG/Os(bpy)<sub>2</sub>PVI-GOx bioanode that enables release of IBU. The control cell without BOx cannot be used for self-powered drug release as it does not provide a sufficient nor a sustained power output, exhibiting decreased power and voltage on consecutive testing (Fig.

S13). This cell when operated at 0.07 V showed negligible levels of release of IBU in comparison to spontaneous release. Further control experiments were performed by coating PEDOT-IBU onto the NPG/Os(bpy)<sub>2</sub>PVI-GOx anode instead of the cathode (Fig. S14). The assembled EBFC showed negligible levels of release of IBU at 0.15 V. These results demonstrate that reduction of the PEDOT-IBU layer (the presence of BOx) is necessary to enable release of IBU.<sup>20</sup>

**Controlled Release of Anionic Fluorescein (FLU) Dye.** The release of FLU, which has been widely used as a model guest molecule,<sup>37-39</sup> was evaluated. Polypyrrole (PPy)<sup>40</sup> has been reported to be more effective than PEDOT for the release of dyes such as FLU, although the basis for this is unclear.<sup>26</sup> Accordingly, a PPy-FLU layer was electrodeposited onto a NPG/Os(bpy)<sub>2</sub>PVI-BOx cathode (Fig. 2A) and the release of FLU was monitored by fluorescence (Fig. S15). The NPG/Os(bpy)<sub>2</sub>PVI-BOx/PPy-FLU biocathode showed a reasonable biocatalytic response towards the reduction of dioxygen, with a  $j_{\text{net}}$  of  $15.3 \pm 0.4 \mu\text{A cm}^{-2}$  at +0.135 V vs. SCE and an onset potential of 0.311 V vs. SCE (Fig. 2B). The presence of FLU in solution posed no inhibitory effects on the performance of the bioelectrodes (Fig. S16). When coupled with a NPG/Os(bpy)<sub>2</sub>PVI-GOx bioanode, the resulting EBFC(2) possessed a  $P_{\max}$  of  $1.14 \mu\text{W cm}^{-2}$  at 0.146 V and an OCV of 0.39 V (Fig. 2C), results comparable to those observed with EBFC(1).

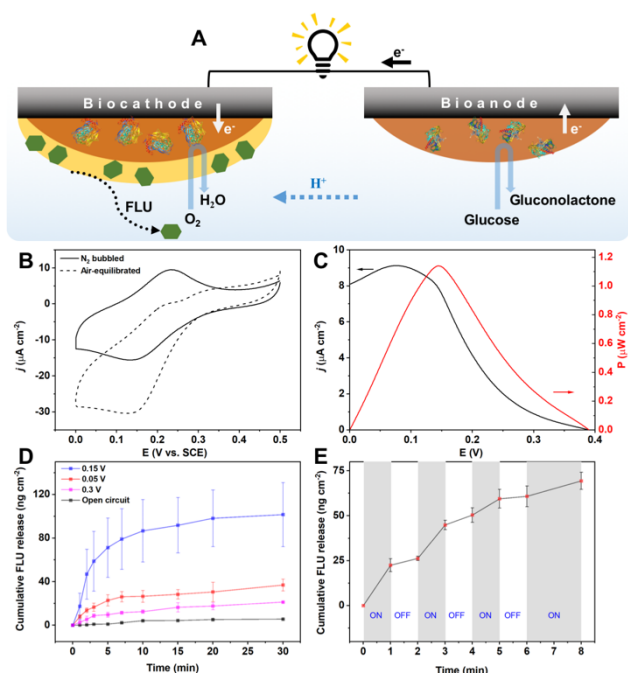


**Figure 2.** (A) Scheme of the controlled FLU release system; CVs of the NPG/Os(bpy)<sub>2</sub>PVI-BOx/PPy-FLU biocathode (B) in 0.1 M pH 7.0 PBS at  $5 \text{ mV s}^{-1}$ ; (C) Power and current density profiles of EBFC(2) consisting of a NPG/Os(bpy)<sub>2</sub>PVI-GOx bioanode and a NPG/Os(bpy)<sub>2</sub>PVI-BOx/PPy-FLU biocathode in air-equilibrated solution containing 10 mM glucose; (D) Cumulative amount of IBU released during the operation of EBFC(2) at various potentials; (E) Cumulative amount of FLU released during the EBFC(2) operating in “on-off” mode: “on” indicates that EBFC(2) was operating at 0.15 V; “off” indicates operating at open-circuit mode (blue line).

The FLU doped PPy layer was reduced at the cathode due to the dioxygen-reduction reaction, enabling the release of FLU (Eq. S2, Fig. 2A). The cumulative amount of FLU released was recorded at a range of potentials (Fig. 2D). Rapid release of FLU occurred in the first 5 min,

when the EBFC was operating at 0.15 V, with equilibrium levels of release attained in ca. 10 min, in contrast to ca. 30 min for IBU. The equilibrium amount of FLU released in solution was  $101.5 \pm 29.3$ ,  $36.9 \pm 5.3$ ,  $21.3 \pm 0.3$  and  $5.6 \pm 0.3$  ng cm<sup>-2</sup> within 25 min for 0.15, 0.05, 0.3 V and for spontaneous release, respectively. This is in agreement with the release of IBU (Fig. 1E) where the maximum amount released was achieved at the same potential as P<sub>max</sub>. The dramatic difference (18-fold) between the amounts of FLU released at 0.15 V and in a spontaneous manner confirmed that an efficient delivery process was feasible with the EBFC based system. The release profile for FLU that was obtained with sequential application of “on” and “off” potentials is further evidence of a controlled release system, as the amount of FLU released attained a plateau during the intermittent “OFF” steps (Fig. 2E).

***In situ* Release of Cationic Fluorophore DAPI in Cell Culture Media.** Finally, the *in situ* release of the cationic fluorophore, DAPI, by an EBFC based system in Dulbecco's modified Eagle medium (DMEM) cell culture media containing ca. 17.5 mM glucose was performed (Fig. 3A). DAPI can be used to stain the nucleus and can be used as a fluorescent probe of the cells. The uptake of the dye by retinal pigment epithelium (RPE) cell lines was investigated using confocal microscopy. In contrast to anionic species such as IBU and FLU, cationic materials such as DAPI can be incorporated into PPy *via* electrostatic interactions and then released when these electrostatic interactions are altered during the redox process.<sup>41</sup> Thompson et al. employed *p*-toluenesulfonate (pTS) as an anionic dopant of PPy to release neurotrophin (cationic).<sup>42</sup> Release of neurotrophin occurred when the redox state of PPy was altered, due to changes in electrostatic interactions between the dopants and PPy.

DAPI was encapsulated into PPy films in the presence of pTS during electropolymerization of a polypyrrole layer on a NPG/Os(bpy)<sub>2</sub>PVI-Box modified electrode. The NPG/Os(bpy)<sub>2</sub>PVI-Box/PPy-pTS-DAPI cathode exhibited a net catalytic current density of  $26.8 \pm 1.9$  μA cm<sup>-2</sup> at 0.17 V vs. SCE undergoing oxygen reduction in air-equilibrated cell culture media (Fig. 3B). The onset potential was 0.35 V vs. SCE. EBFC(3) generated a P<sub>max</sub> of 2.05 μW cm<sup>-2</sup> at 0.135 V with an OCV of 0.387 V in

the same medium (Fig. 3C). *Ex situ* release of DAPI in PBS at 0.15 V was observed, with an initial fast rate of release for 20 min, attaining an equilibrium value within 90 min (Fig. S17 and S18). The amount of DAPI released at a potential of 0.15 V was  $102.5 \pm 10.5$  ng cm<sup>-2</sup>, 6 times higher than that observed by spontaneous release (Fig. S18), demonstrating that controlled delivery could be achieved with this system.

*In situ* release of DAPI by the EBFC(3) operating at 0.15 V was conducted in cell culture media with incubated RPE cells for 30 min. Confocal microscopic images showed blue-fluorescent RPE cells when excited at 405 nm, indicating the successful cellular uptake of permeable DAPI (Fig. 3D and 3E). This also implies that the structure of DAPI was unaffected by the EBFC based drug release system. Conversely, a negative control with open-circuit potential release of the EBFC(3) resulted in a very low density of stained RPE cells (Fig. 3F and 3G). The morphology of the cells was unchanged in the presence of the EBFC(3), indicating that the system showed a high degree of biocompatibility *in vitro* (Fig. 3D and 3F).

CellTrace™ Yellow, which can be retained by cell membranes, was used to label all cells in a particular field of view and imaged by fluorescence microscopy (excited at 543 nm). Characterisation of the successful staining of cell nuclei was based on the detection of cell labelling by cell trackers and identification of nuclear associated fluorescence intensity of DAPI at 405 nm. Quantitative analysis of five random areas with more than 100 cells per FOV was performed. Fig. 3H illustrates the positive labeling to similar levels of cells by cell trace in both control and loaded conditions. In contrast, nuclear labelling associated with DAPI fluorescence was significantly enriched when EBFC(3) was operating at 0.15 V. Similar results are observed when assessing DAPI staining in isolation. This was further verified by comparing the overall fluorescence intensity of DAPI per FOV for the loaded and unloaded control ( $18.7 \pm 3.0$  vs.  $3.5 \pm 1.5$ ) (Fig. 3I). A t-value of 4.561 (P < 0.01) with a degree of freedom of 8 was obtained from the unpaired two tailed student's t-Test, confirming a statistically significant difference between the loaded and unloaded control. Thus, *in vitro* experiments established the viability and effectiveness of the EBFC based controlled drug release approach.

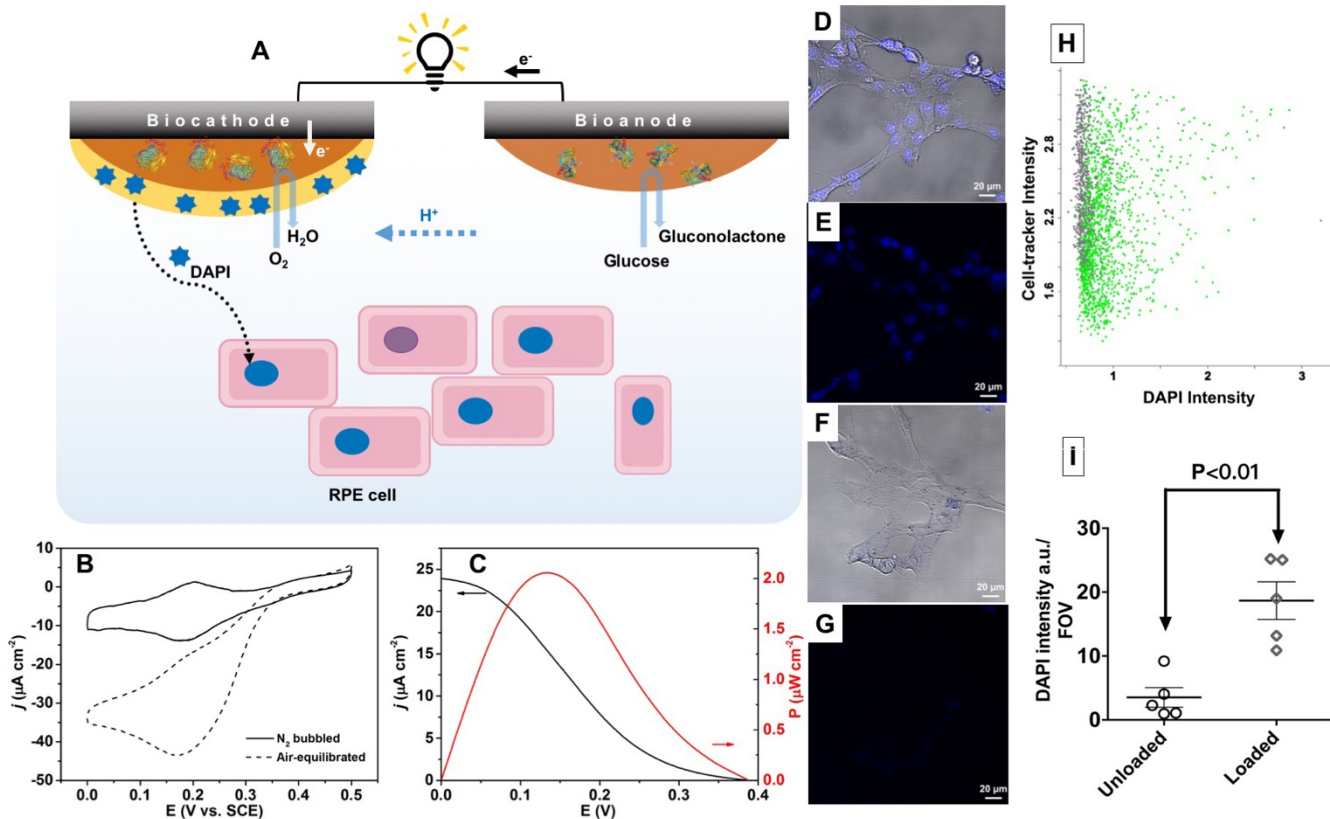


**Figure 3.** (A) Scheme of *in situ* DAPI release in a cell culture medium; (B) CVs of the NPG/Os(bpy)<sub>2</sub>PVI-BOx/PPy-pTS-DAPI biocathode in cell culture media (5 mV s<sup>-1</sup>); (C) Power and current density profiles of the EBFC(3) consisting of a NPG/Os(bpy)<sub>2</sub>PVI-GOx bioanode and a NPG/Os(bpy)<sub>2</sub>PVI-BOx/PPy-pTS-DAPI biocathode in air-equilibrated cell culture media; (D-G). Confocal fluorescence images of RPE cells after incubation in the cell culture media with the EBFC(3) operation at 0.15 V (D, E) and open circuit for 30 min (F, G): (D, F) overlay images of the Blue fluorescence channel and transmission images, (E, G) Blue fluorescence images; scale bar: 20 μm. (H) Scatter-plot of the fluorescence intensity of cell-tracker vs. DAPI intensity; Green and grey columns correspond to the positive and negative control. (I) The plot of DAPI intensity per FOV. Values were represented as the mean (horizontal lines) ± standard error of the mean of five separate experiments (circles).

## CONCLUSIONS

In summary, a self-powered, controlled drug release system, based on bi-layer modified electrodes has been demonstrated. Three model compounds, bearing negative, neutral or positive charges were released in a controlled manner *ex situ*. The maximum amounts released depended on the power density of the EBFC. The blue fluorophore DAPI was encapsulated in polypyrrole and released from an EBFC system to efficiently stain RPE cells, indicating that the system was biocompatible<sup>43</sup>. The approach is of interest for use with other redox enzymes and fuels and for feasibility of miniaturisation. The preliminary results demonstrate possible applications of the EBFC based system for “on demand” implantable drug release system. Further evaluation of the suitability of the approach described will require examining the stability and response of the cell after sterilization and on implantation in tissue.

## EXPERIMENTAL SECTION

**Materials.** D-(+)-glucose (99.5%), 3,4-ethylenedioxythiophene (EDOT, 97%), pyrrole (98%), GOx from *Aspergillus niger* (EC 1.1.3.4, type II, ≥15,000 U g<sup>-1</sup>), sodium phosphate (monobasic dehydrate ≥99% and dibasic ≥99%), ibuprofen sodium salt (IBU, ≥98%), polyethylene glycol 3400 (PEG3400), fluorescein sodium salt (FLU), sodium p-toluenesulfonate (pTS, 95%), Dulbecco's modified Eagle's medium/nutrient mixture F-12 Ham (DMEM:F12 HAM (1:1 v/v)), sodium bicarbonate, antibiotic-antimycotic solutions, hygromycin, paraformaldehyde (PFA), 2,2'-azino-bis (3-ethylbenzothiazoline-6-sulfonic acid) diammonium salt (ABTS) and sulfuric acid (H<sub>2</sub>SO<sub>4</sub>, 95-98%)

were obtained from Sigma-Aldrich Ireland, Ltd. CellTrace™ Yellow and 4',6-diamidino-2-phenylindole (DAPI) were purchased from Thermo Fisher Scientific. *Myrothecium verrucaria* BOx (EC 1.3.3.5, 2.63 U mg<sup>-1</sup>) was from Amano Enzyme Inc., Japan. Os(bpy)<sub>2</sub>PVI was synthesised via an established procedure<sup>44-45</sup>. Deionised water (18.2 MΩ cm, Elga Purelab Ultra, UK) was used to prepare all the solutions.

Nanoporous gold (NPG, pore size ca. 30 nm) modified electrodes were prepared as described previously.<sup>12,27</sup> 100 nm thick Au/Ag leaf alloy leaves (12-carat, Eytzinger, Germany) were dealloyed in concentrated HNO<sub>3</sub> (Sigma-Aldrich) for 30 min at 30 °C. The resulting NPG films were then attached onto pre-polished glassy carbon electrodes (GCEs, diameter: 4 mm). Cyclic voltammetry (CV) of NPG in 1 M H<sub>2</sub>SO<sub>4</sub> for 15 cycles were performed to create clean surfaces and left to dry naturally.

**Bioelectrode Construction and Drug Loading.** NPG/Os(bpy)<sub>2</sub>PVI-GOx and NPG/Os(bpy)<sub>2</sub>PVI-BOx bioelectrodes were prepared separately. A 5.3 μl aliquot of a 6 mg ml<sup>-1</sup> aqueous suspension of Os(bpy)<sub>2</sub>PVI, was combined with 1.3 μl of a 15 mg ml<sup>-1</sup> aqueous solution of PEGDGE and 3.2 μl of a 10 mg ml<sup>-1</sup> solution of either GOx or BOx. All the components were homogenously mixed by vortexing. The surface of the NPG electrode was fully covered by a drop of the solution, and immediately placed in a vacuum desiccator connected to a vacuum pump for 10 min. The electrodes were then placed in a refrigerator and allowed to dry overnight in the dark at 4°C.

To load IBU, a second layer of PEDOT doped with IBU was subsequently electrodeposited onto the NPG/Os(bpy)<sub>2</sub>PVI-BOx biocath-

ode, resulting in NPG/Os(bpy)<sub>2</sub>PVI-BOx/PEDOT-IBU. An electro-deposition solution containing PBS (0.1 M, pH 7.0), 2 mM polyethylene glycol 3400 (PEG3400), 20 mM EDOT and 10 mM IBU was used. Electrodeposition was performed using pulse sequence comprised of 0.9 V (2 s) and -0.4 V (3 s) for a total time of 300 s. The oxidation potential of 0.9 V was based on the cyclic voltammograms for the electropolymerization of EDOT (Fig. S1). The electrodes were then soaked in PBS for 30 min to remove any loosely attached IBU. The IBU loading in the PEDOT-IBU film was estimated by the concentration difference of IBU in the electropolymerization electrolyte before and after electropolymerization. In order to perform spectroscopic studies of the PEDOT-IBU layer, the same procedure was employed to coat Os(bpy)<sub>2</sub>PVI-BOx/PEDOT-IBU onto an indium tin oxide coated glass (ITO) or gold foil. Enzymatic activity of the immobilized BOx was monitored by soaking the electrodes in 2 mL of air-equilibrated 50 μM ABTS for 5 min, and the absorbance at 420 nm monitored. The absorbance reached 0.462±0.153 and 0.318±0.008 for NPG/Os(bpy)<sub>2</sub>PVI-BOx and NPG/Os(bpy)<sub>2</sub>PVI-BOx/PEDOT-IBU, respectively.

To load FLU, a second layer of PPy doped with FLU was electrodeposited onto NPG/Os(bpy)<sub>2</sub>PVI-BOx, resulting in NPG/Os(bpy)<sub>2</sub>PVI-BOx/PPy-FLU. An electro-deposition solution containing 0.1 M pH 7.0 PBS with 20 mM PPy and 50 μM FLU was prepared. A 60 s pulse sequence (0.9 V (2 s) and -0.4 V (3 s)) was applied. The electrodes were then gently rinsed with PBS for 30 min.

For the biocathode, a second layer of PPy doped with pTS and DAPI was electrodeposited onto NPG/Os(bpy)<sub>2</sub>PVI-BOx, leading to NPG/Os(bpy)<sub>2</sub>PVI-BOx/PPy-pTS-DAPI. The electro-deposition solution contained 0.1 M pH 7.0 PBS with 25 mM PPy, 0.1 M pTS and 200 μM DAPI. A 60 s pulse sequence comprising 0.9 V (2 s) and -0.4 V (3 s) was used. Physically adsorbed DAPI was removed by immersing the electrodes in PBS for 30 min.

**Morphology and Composition Characterisation.** Scanning electron microscopy (SEM, Hitachi SU-70, 20 kV) and transmission electron microscopy (TEM, Tecnai G2 T20, 200 kV) were used to characterise the electrode surface. The thicknesses of the modification layers were estimated using TEM, using the contrast difference between the gold skeleton and the coating layers. The average pore size of NPG and deposition layer thickness were obtained by measuring at least 30 times with ImageJ software (National Institutes of Health, Bethesda, Maryland)<sup>46</sup>. Fourier transform infrared spectroscopy (FTIR) measurements of the composite layers were performed using a Bruker Optics Alpha-P spectrometer. Gold foils (thickness: 0.1 mm, purity: 99.9%) were used as the substrate for polymer modification. ITO coated glass slides were used to support NPG for atomic force microscopic (AFM) characterisation using a 5500 SPM system (Keysight Technologies, Santa Rosa CA, USA) in tapping mode.

#### 1.4. Electrochemical Measurements

Electrochemical characterisation was carried out using a CHI802 potentiostat (CH Instruments, Austin, Texas) with a three-electrode system composed of NPG based working electrodes, a saturated calomel electrode (SCE) as the reference electrode and a platinum counter electrode. Cyclic voltammetry was employed to characterise the modified electrodes and the electrochemical capacitance of the electrode was calculated from the current densities at 0.4 V vs. SCE when there was no faradaic process involved. The net catalytic currents were determined by subtracting the background currents obtained from the blank CVs from the electrocatalytic currents.

The assembled enzymatic biofuel cells (EBFCs) were analysed in a two-electrode system by using a NPG/Os(bpy)<sub>2</sub>PVI-GOx bioanode as the working electrode and various NPG/Os(bpy)<sub>2</sub>PVI-BOx based modified biocathodes as the combined counter/reference electrode. To

distinguish between the EBFCs, EBFC(1), EBFC(2) and EBFC(3) denote EBFC comprised of NPG/Os(bpy)<sub>2</sub>PVI-BOx/PEDOT-IBU, NPG/Os(bpy)<sub>2</sub>PVI-BOx/PPy-FLU and NPG/Os(bpy)<sub>2</sub>PVI-BOx/PPy-pTS-DAPI, respectively. The current in the potential range between the open circuit voltage (OCV) of the EBFC and 0 V at 1 mV s<sup>-1</sup> was recorded, and subsequently used to generate a power density profile. During recording of the polarisation curve of the assembled EBFC, the potential of the biocathode ( $E_{\text{biocathode}}$  in V vs. SCE) was monitored independently using an additional potentiostat (PalmSens 3, The Netherlands) by connecting the working electrode and counter electrode to the biocathode and a SCE reference electrode, respectively. The potential of the bioanode ( $E_{\text{bioanode}}$  in V vs. SCE) is determined by the voltage difference between the potential of the biocathode and the corresponding cell voltage of the EBFC ( $E_{\text{cell}}$  in V), i.e.  $E_{\text{cell}} = E_{\text{biocathode}} - E_{\text{bioanode}}$ .

**Drug Release Studies.** The release of IBU, FLU and DAPI from the electrodes was carried out under open circuit mode (spontaneous release) or EBFC-triggered mode in 1 mL air-equilibrated 0.1 M pH 7.0 PBS containing 10 mM glucose, respectively. The release of IBU from NPG/Os(bpy)<sub>2</sub>PVI-BOx/PEDOT-IBU at different voltages was carried out with a three-electrode system in 1 mL air-equilibrated 0.1 M pH 7.0 PBS. The cumulative release of IBU in solution was monitored at 222 nm using a Cary 60 UV-Vis spectrophotometer (Agilent, USA). A calibration curve by plotting standard IBU concentration versus absorbance at 222 nm was obtained. Cumulative release of FLU was monitored using an Agilent Cary Eclipse fluorescence spectrophotometer (Germany) with excitation at 460 nm. A calibration curve was obtained from the emission intensity at 515 nm. The concentration of DAPI released in the solution was also measured by the fluorescence spectrophotometer with excitation at 340 nm, collecting emission intensity at 488 nm. Based on these calibration curves, the normalised amounts (nmol cm<sup>-2</sup> or μmol cm<sup>-2</sup>) of IBU, FLU and DAPI released were determined.

**In situ Release of DAPI.** RPE1 cells (ATCC CRL-4000) were maintained at 37°C, 5% CO<sub>2</sub>, in complete medium (DMEM:F12 HAM (1:1 v/v) supplemented with 10% fetal bovine serum (FBS, ThermoFisher), 0.5% (w/v) sodium bicarbonate, 2 mM GlutaMAX (Life Technologies), antibiotic-antimycotic, and 20 μg mL<sup>-1</sup> hygromycin). To perform the assay, cells were seeded in 6 well culture dishes at a seeding density of 1 x 10<sup>6</sup> cells/mL and maintained for 48 h prior to experimentation. An EBFC consisting of a NPG/Os(bpy)<sub>2</sub>PVI-GOx bioanode and a NPG/Os(bpy)<sub>2</sub>PVI-BOx/PPy-DAPI biocathode was incubated in a 1 mL culturing medium and operated at 0.15 V for 0.5 h. 1 μM CellTrace™ Yellow was used to label the cells for 15 min. The stained cells were then washed in PBS followed by fixation with 4% PFA in PBS for 15 min at room temperature. Fluorescently labelled images were acquired by confocal microscopic (Zeiss LSM 710; Carl Zeiss).

**Image and Statistical Analysis.** Images acquired were analyzed by an analysis pipeline created in the CellProfiler image analysis software. RPE1 cells were denoted by CellTrace™ Yellow and DAPI labelling. Each image-set corresponded to 5 fields of view (FOV) with over 100 cells per FOV.

In brief, effects of variation of illumination were corrected using an illumination correction function for each channel using a median filter (50 x 50 pixels). Each image was processed by firstly segmenting the cell boundaries by CellTrace™ Yellow labelling using an arbitrary fluorescence intensity corresponding to the red fluorescent channel. Next, nuclear labelling within this segmented image was identified using DAPI labelling corresponding to an arbitrary fluorescence intensity, median size (20 to 60 pixels) and shape (circular). Identified cells objects were then measured by their mean fluorescence intensity in both DAPI and

cell tracker channels associated with the identified segmented cell regions. Data was either expressed as a median per image or as an amalgamation of all images.

GraphPad Prism 5 software was used to undertake the statistical analysis (GraphPad Software Inc., La Jolla, CA). For comparison of two groups, an unpaired two tailed student's t-Test was undertaken and instances of  $P < 0.05$  were statistically significant (\* $P < 0.05$ ; \*\* $P < 0.01$ ; \*\*\* $P < 0.001$ ). All values are reported as the mean  $\pm$  standard error of the mean.

## ASSOCIATED CONTENT

### Supporting Information

Details of bioelectrode preparation and characterizing data, supplementary figures and tables. The Supporting Information is available free of charge on the ACS Publications website.

## AUTHOR INFORMATION

### Corresponding Author

\*Xinxin Xiao, E-mail: xinxin.xiao@ul.ie, xixiao@kemi.dtu.dk;

\*Edmond Magner, E-mail: edmond.magner@ul.ie; Fax: +353 61 213529; Tel: +353 61 234390

### Notes

The authors declare no competing financial interests.

## ACKNOWLEDGMENT

This work was financially supported by the European Commission (FP7-PEOPLE-2013-ITN 607793 "Bioenergy"). X. Xiao acknowledges an IRC Postgraduate Scholarship (GOIPG/2014/659) and a H. C. Ørsted COFUND fellowship. Funding from the Programme for Research in Third-Level Institutions (PRTL) cycles 4 and 5 is acknowledged. K.D. McGourty acknowledges a Health Research Institute Seed Funding Award from University of Limerick (UL). We thank Prof. Dónal Leech and Dr. Peter Ó Conghaile from the National University of Ireland Galway for providing osmium redox polymers. Prof. Jens Ulstrup is acknowledged for proof reading.

## REFERENCES

- Leech, D.; Kavanagh, P.; Schuhmann, W., Enzymatic fuel cells: recent progress. *Electrochim. Acta* **2012**, *84* (0), 223-234.
- Rasmussen, M.; Abdellaoui, S.; Minteer, S. D., Enzymatic biofuel cells: 30 years of critical advancements. *Biosens. Bioelectron.* **2015**, *76*, 91-102.
- Xiao, X.; Xia, H.-q.; Wu, R.; Bai, L.; Yan, L.; Magner, E.; Cosnier, S.; Lojou, E.; Zhu, Z.; Liu, A., Tackling the challenges of enzymatic (bio)fuel cells. *Chem. Rev.* **2019**, *119* (16), 9509-9558.
- Göbel, G.; Beltran, M. L.; Mundhenk, J.; Heinlein, T.; Schneider, J.; Lisdat, F., Operation of a carbon nanotube-based glucose/oxygen biofuel cell in human body liquids-Performance factors and characteristics. *Electrochim. Acta* **2016**, *218*, 278-284.
- Calabrese Barton, S.; Galloway, J.; Atanassov, P., Enzymatic biofuel cells for implantable and microscale devices. *Chem. Rev.* **2004**, *104* (10), 4867-4886.
- Gamella, M.; Koushanpour, A.; Katz, E., Biofuel cells – activation of micro- and macro-electronic devices. *Bioelectrochem.* **2018**, *119* (Supplement C), 33-42.
- Cosnier, S.; Le Goff, A.; Holzinger, M., Towards glucose biofuel cells implanted in human body for powering artificial organs: review. *Electrochem. Commun.* **2014**, *38*, 19-23.
- Mark, A. G.; Suraniti, E.; Roche, J.; Richter, H.; Kuhn, A.; Mano, N.; Fischer, P., On-chip enzymatic microbiofuel cell-powered integrated circuits. *Lab Chip* **2017**, *17* (10), 1761-1768.
- Conzuelo, F.; Ruff, A.; Schuhmann, W., Self-powered bioelectrochemical devices. *Curr. Opin. Electrochem.* **2018**, *12*, 156-163.
- Grattieri, M.; Minteer, S. D., Self-powered biosensors. *ACS Sens.* **2018**, *3* (1), 44-53.
- Katz, E.; Bückmann, A. F.; Willner, I., Self-Powered Enzyme-Based Biosensors. *J. Am. Chem. Soc.* **2001**, *123* (43), 10752-10753.
- Xiao, X.; Conghaile, P. Ó.; Leech, D.; Ludwig, R.; Magner, E., A symmetric supercapacitor/biofuel cell hybrid device based on enzyme-modified nanoporous gold: An autonomous pulse generator. *Biosens. Bioelectron.* **2017**, *90*, 96-102.
- Agnes, C.; Holzinger, M.; Le Goff, A.; Reuillard, B.; Elouarzaki, K.; Tingry, S.; Cosnier, S., Supercapacitor/biofuel cell hybrids based on wired enzymes on carbon nanotube matrices: autonomous reloading after high power pulses in neutral buffered glucose solutions. *Energy Environ. Sci.* **2014**, *7* (6), 1884-1888.
- Lu, Y.; Aimetti, A. A.; Langer, R.; Gu, Z., Bioresponsive materials. *Nat. Rev. Mater.* **2016**, *2*, 16075.
- Zhang, S.; Bellinger, A. M.; Glettig, D. L.; Barman, R.; Lee, Y.-A. L.; Zhu, J.; Cleveland, C.; Montgomery, V. A.; Gu, L.; Nash, L. D.; Maitland, D. J.; Langer, R.; Traverso, G., A pH-responsive supramolecular polymer gel as an enteric elastomer for use in gastric devices. *Nat. Mater.* **2015**, *14*, 1065.
- Uhrich, K. E.; Cannizzaro, S. M.; Langer, R. S.; Shakesheff, K. M., Polymeric systems for controlled drug release. *Chem. Rev.* **1999**, *99* (11), 3181-3198.
- Okhokhonin, A. V.; Domanskyi, S.; Filipov, Y.; Gamella, M.; Kozitsina, A. N.; Privman, V.; Katz, E., Biomolecular release from alginate-modified electrode triggered by chemical inputs processed through a biocatalytic cascade – integration of biomolecular computing and actuation. *Electroanalysis* **2017**, *30* (3), 426-435.
- Mailloux, S.; Halámek, J.; Halámková, L.; Tokarev, A.; Minko, S.; Katz, E., Biomolecular release triggered by glucose input – bioelectronic coupling of sensing and actuating systems. *Chem. Commun.* **2013**, *49* (42), 4755-4757.
- Mailloux, S.; Halámek, J.; Katz, E., A model system for targeted drug release triggered by biomolecular signals logically processed through enzyme logic networks. *Analyst* **2014**, *139* (5), 982-986.
- Zhou, M.; Zhou, N.; Kuralay, F.; Windmiller, J. R.; Parkhomovsky, S.; Valdés-Ramírez, G.; Katz, E.; Wang, J., A self-powered "sense-act-treat" system that is based on a biofuel cell and controlled by Boolean logic. *Angew. Chem. Int. Ed.* **2012**, *51* (11), 2686-2689.
- Ogawa, Y.; Kato, K.; Miyake, T.; Nagamine, K.; Ofuji, T.; Yoshino, S.; Nishizawa, M., Organic transdermal iontophoresis patch with built-in biofuel cell. *Adv. Healthc. Mater.* **2015**, *4* (4), 506-510.
- Heinze, J.; Frontana-Urbe, B. A.; Ludwigs, S., Electrochemistry of Conducting Polymers—Persistent Models and New Concepts. *Chem. Rev.* **2010**, *110* (8), 4724-4771.
- Uppalapati, D.; Boyd, B. J.; Garg, S.; Travas-Sejdic, J.; Svirskis, D., Conducting polymers with defined micro- or nanostructures for drug delivery. *Biomaterials* **2016**, *111*, 149-162.
- Svirskis, D.; Travas-Sejdic, J.; Rodgers, A.; Garg, S., Electrochemically controlled drug delivery based on intrinsically conducting polymers. *J. Controlled Release* **2010**, *146* (1), 6-15.
- Alshammary, B.; Walsh, F. C.; Herrasti, P.; Ponce de Leon, C., Electrodeposited conductive polymers for controlled drug release: polypyrrole. *J. Solid State Electrochem.* **2016**, *20* (4), 839-859.
- Winther-Jensen, B.; Clark, N. B., Controlled release of dyes from chemically polymerised conducting polymers. *React. Funct. Polym.* **2008**, *68* (3), 742-750.
- Xiao, X.; Conghaile, P. Ó.; Leech, D.; Ludwig, R.; Magner, E., An oxygen-independent and membrane-less glucose biobattery/supercapacitor hybrid device. *Biosens. Bioelectron.* **2017**, *98*, 421-427.
- Xiao, X.; Si, P.; Magner, E., An overview of dealloyed nanoporous gold in bioelectrochemistry. *Bioelectrochemistry* **2016**, *109*, 117-126.
- Xiao, X.; Ulstrup, J.; Li, H.; Zhang, J.; Si, P., Nanoporous gold assembly of glucose oxidase for electrochemical biosensing. *Electrochimica Acta* **2014**, *130*, 559-567.
- Krukiewicz, K.; Zak, J. K., Conjugated polymers as robust carriers for controlled delivery of anti-inflammatory drugs. *J. Mater. Sci.* **2014**, *49* (16), 5738-5745.
- Xiao, X.; Siepenkoetter, T.; Conghaile, P. Ó.; Leech, D.; Magner, E., Nanoporous gold-based biofuel cells on contact lenses. *ACS Appl. Mater. Interfaces* **2018**, *10* (8), 7107-7116.
- Conzuelo, F.; Marković, N.; Ruff, A.; Schuhmann, W., The open circuit voltage in biofuel cells: Nernstian shift in pseudocapacitive electrodes. *Angew. Chem. Int. Ed.* **2018**, *57* (41), 13681-13685.

33. Pankratov, D.; Conzuelo, F.; Pinyou, P.; Alsaoub, S.; Schuhmann, W.; Shleev, S., A Nernstian Biosupercapacitor. *Angew. Chem. Int. Ed.* **2016**, *55* (49), 15434-15438.
34. Chen, H.; Prater, M. B.; Cai, R.; Dong, F.; Chen, H.; Minteer, S. D., Bioelectrocatalytic Conversion from N<sub>2</sub> to Chiral Amino Acids in a H<sub>2</sub>/α-Keto Acid Enzymatic Fuel Cell. *J. Am. Chem. Soc.* **2020**, *142* (8), 4028-4036.
35. Marzocchi, M.; Gualandi, I.; Calienni, M.; Zironi, I.; Scavetta, E.; Castellani, G.; Fraboni, B., Physical and electrochemical properties of PEDOT:PSS as a tool for controlling cell growth. *ACS Appl. Mater. Interfaces* **2015**, *7* (32), 17993-18003.
36. Chen, X.; Inganäs, O., Three-step redox in polythiophenes: evidence from electrochemistry at an ultramicroelectrode. *J. Phys. Chem.* **1996**, *100* (37), 15202-15206.
37. Giri, S.; Trewyn, B. G.; Stellmaker, M. P.; Lin, V. S. Y., Stimuli-responsive controlled-release delivery system based on mesoporous silica nanorods capped with magnetic nanoparticles. *Angew. Chem. Int. Ed.* **2005**, *44* (32), 5038-5044.
38. Luo, X.; Cui, X. T., Electrochemically controlled release based on nanoporous conducting polymers. *Electrochem. Commun.* **2009**, *11* (2), 402-404.
39. Seker, E.; Berdichevsky, Y.; Staley Kevin, J.; Yarmush Martin, L., Microfabrication - compatible nanoporous gold foams as biomaterials for drug delivery. *Adv. Healthc. Mater.* **2012**, *1* (2), 172-176.
40. George, P. M.; LaVan, D. A.; Burdick, J. A.; Chen, C. Y.; Liang, E.; Langer, R., Electrically controlled drug delivery from biotin - doped conductive polypyrrole. *Adv. Mater.* **2006**, *18* (5), 577-581.
41. Szunerits, S.; Teodorescu, F.; Boukherroub, R., Electrochemically triggered release of drugs. *Eur. Polym. J.* **2016**, *83*, 467-477.
42. Thompson, B. C.; Moulton, S. E.; Ding, J.; Richardson, R.; Cameron, A.; O'Leary, S.; Wallace, G. G.; Clark, G. M., Optimising the incorporation and release of a neurotrophic factor using conducting polypyrrole. *J. Controlled Release* **2006**, *116* (3), 285-294.
43. Lee, J. H.; Jeon, W.-Y.; Kim, H.-H.; Lee, E.-J.; Kim, H.-W., Electrical stimulation by enzymatic biofuel cell to promote proliferation, migration and differentiation of muscle precursor cells. *Biomaterials* **2015**, *53*, 358-369.
44. Kober, E. M.; Caspar, J. V.; Sullivan, B. P.; Meyer, T. J., Synthetic routes to new polypyridyl complexes of osmium(II). *Inorg. Chem.* **1988**, *27* (25), 4587-4598.
45. Forster, R. J.; Vos, J. G., Synthesis, characterization, and properties of a series of osmium- and ruthenium-containing metallopolymers. *Macromolecules* **1990**, *23* (20), 4372-4377.
46. Schneider, C. A.; Rasband, W. S.; Eliceiri, K. W.; Schindelin, J.; Arganda-Carreras, I.; Frise, E.; Kaynig, V.; Longair, M.; Pietzsch, T.; Preibisch, S., NIH image to imagej: 25 years of image analysis. *Nat. Methods* **2012**, *9* (7), 671.

